JBC Papers in Press. Published on January 14, 2011 as Manuscript M110.152181
The latest version is at http://www.jbc.org/cgi/doi/10.1074/jbc.M110.152181

Plasminogen/Plasmin modulates bone metabolism by regulating the osteoblast and osteoclast function.

Running Title Plasminogen/Plasmin modulates bone metabolism

Yosuke Kanno[1], Akira Ishisaki[2], Eri Kawashita[1], Naoyuki Chosa[2], Keiichi Nakajima[3], Tatsuji Nishihara[4], Kuniaki Toyoshima[5], Kiyotaka Okada[6], Shigeru Ueshima[6, 7], Kenji Matsushita[8], Osamu Matsuo[6], Hiroyuki Matsuno[1]

1. Department of Clinical Pathological Biochemistry, Faculty of Pharmaceutical Science, Doshisha Women's Collage of Liberal Arts, 97-1 Kodo Kyo-tanabe, Kyoto 610-0395, Japan.
2. Department of Biochemistry, Iwate Medical University School of Dentistry, 1-3-27, Chuo-dori, Morioka, Iwate 020-8505, Japan.
3. Department of Animal Production and Grassland, National Agricultural Research Center for Hokkaido Region, Sapporo, Japan.
4. Division of Infections and Molecular Biology, Department of Health Promotion, Kyushu Dental College, 2-6-1 Manazuru, Kokurakita-ku, Kitakyushu 803-8580, Japan.
5. Division of Oral Histology and Neurobiology, Department of Biosciences, Kyushu Dental College, 2-6-1 Manazuru, Kokurakita-ku, Kitakyushu 803-8580, Japan.
6. Department of Physiology II. Kinki University School of Medicine 377-2 Ohnohigashi, Osaka-sayama-city 589-8511, Japan.
7. Department of Food Science and Nutrition, Kinki University School of Agriculture, Nara, 631-8505, Japan
8. Laboratory of Oral Disease Research, National Institute for Longevity Sciences, National Center for Geriatrics and Gerontology, 36-3 Gengo, Morioka, Obu, Aichi 474-8522, Japan.

Corresponding Author:

Yosuke Kanno, Dept. of Clinical Pathological Biochemistry, Faculty of Pharmaceutical Science, Doshisha Women's Collage of Liberal Arts, 97-1 Kodo Kyo-tanabe 610-0395 Kyoto, Japan Telephone +81-0774-65-8629; Fax +81-0774-65-8479; E-mail: ykanno@dwc.doshisha.ac.jp

The contribution of plasminogen (Plg)/plasmin which have been claimed to be the main fibrinolytic regulators in the bone metabolism remains unclear. This study evaluated how the absence of Plg affects the function of osteoblast (OB) and osteoclast (OC). There was a larger population of pre-OCs in bone marrow-derived cells from the $Plg^{-/-}$ mice than the population of that from the WT mice. In addition, the absent of Plg suppressed the expression of osteoprotegerin (OPG) in OBs. Moreover, an exogenous plasmin clearly induced the OPG expression in $Plg^{-/-}$ OBs. On the other hand, the osteoclastogenesis of RAW264.7 mouse monocyte/macrophage lineage cells in coculture with OBs from the $Plg^{-/-}$ mice was significantly accelerated in comparison to that in co-culture with OBs from the WT mice. Intriguingly, the accelerated OC differentiation of RAW264.7 cells co-cultured with $Plg^{-/-}$ OBs was clearly suppressed by the treatment of an exogenous plasmin. Consequently, $Plg^{-/-}$ mice display decreased bone mineral density. These findings could eventually lead to the development of new clinical therapies for bone disease caused by a disorder of the fibrinolytic system.

The fibrinolytic system contains plasminogen (Plg) a proenzyme, which is converted to the active serine protease plasmin, a main component of the fibrinolytic system, through the action of a tissue-type plasminogen activator (tPA) or urokinase-type PA (uPA). The inhibition of the system may occur through the neutralization of the plasminogen activators or plasmin, and this neutralization is achieved mainly by the plasminogen activator inhibitor-1 (PAI-1) or α2-antiplasmin (α2AP), respectively. PAI-1, the primary endogenous inhibitor of tPA or uPA, plays an important role in inhibiting arterial clot lysis (1). On the other hand, α2AP rapidly inactivates plasmin, resulting in the formation of a stable inactive complex, plasmin-α2AP (2). Apart from the removal of fibrin, the fibrinolytic system also plays a pivotal role in such phenomena as embryogenesis, proliferation, migration, wound healing, fibrosis, and tumorigenesis (3-9).

It is suggested that fibrinolytic factors such as tPA, uPA, uPA receptor (uPAR) and PAI-1 are involved in the bone metabolism as follows: The absence of tPA and uPA enhanced OB differentiation and formation of a mineralized bone matrix, and increased bone formation and bone mass (10). On the other hand, the absence of PAI-1 protects against trabecular bone loss induced by estrogen deficiency, suggesting a site-specific

role for PAI-1 in bone turnover (11). In addition, uPAR-lacking mice displayed increased bone mineral density (BMD), increased osteogenic potential of OBs, decreased OCs formation, and cytostkeletal reorganization in mature OCs (12). However, the physiological roles of fibrinolytic main regulators such as Plg/plasmin in bone metabolism are not precisely understood.

The receptor activator of NF-κB (RANK), its ligand RANKL and osteoprotegerin (OPG) control OCs function (13,14). RANK activated by RANKL has proven to be absolutely required for OCs development (15). RANKL is neutralized by OPG that specifically binds to RANKL. OPG is expressed in many tissues apart from OBs, including heart, kidney, liver, spleen, and bone marrow (13). However, molecular mechanisms of OPG expression remain to be elucidated.

We herein report the crucial role of fibrinolytic main regulators Plg/plasmin in bone metabolism especially on the point of view that how the regulators affects the ability of pre-OCs in bone marrow to differentiate into OCs, that of OBs to induce OC differentiation, and that of OBs to mineralize extra-cellular matrix (ECM).

Materials and Methods

All experiments were performed in accordance with the Guide for the Care and Use of Laboratory Animals published by the US National Institutes of Health.

Animals

The Plg deficient ($Plg^{-/-}$) mice (16) were kindly provided by Prof. D Collen (University of Leuven, Belgium).

Wild type (WT) and $Plg^{-/-}$ mice littermates were housed in groups of two to five in filter-top cages with a fixed 12 hours light, 12 hours dark cycle. The body weights of mice were measured weekly.

Reagents

Plasmin, aprotinin, α2AP, epsilon amino caproic acid (EACA) and other chemical substances were obtained from Sigma Chemical (St Louis, MO USA).

Cell culture

Bone marrow cells, RAW264.7 mouse monocyte/macrophage lineage cells (American Type Culture Collection) and primary OBs were maintained in α-MEM (Invitrogen, Carlsbad, CA USA) supplemented with 10% fetal bovine serum (FBS) (Hyclone, Logan, UT USA) and 1% penicillin-streptomycin (Invitrogen, Carlsbad, CA USA) at 37 ℃ in a humidified

atmosphere of 5 % CO_2 / 95 % air.

Primary OBs derived from mice calvaria were obtained as previously described (17).

OC differentiation assay

Bone marrow-derived cells that include a population of pre-OCs were obtained from tibia of 5- to 7-weeks old adult mice. Mouse bone marrow cells were cultured for 3 days with RANKL (100 ng/ml) and M-CSF (100 ng/ml) in 48-well plates. In other experiments, Raw 264.7 cells were co-cultured with OBs from the $Plg^{+/+}$ and $Plg^{-/-}$ mice for 3 days in the absence or presence of interleukin-1β (IL-1β) (5 ng/ml) or prostaglandin E_2 (PGE_2) (1 μM) in 48-well plates. Cells were then fixed and stained for tartrate-resistant acid phosphatase (TRAP; a marker enzyme of OCs) as described (17). TRAP-positive multinucleated cells containing three or more nuclei were counted as OCs, under microscopic examination.

Bone resorption assay

To estimate bone resorption activity of differentiated OCs from bone marrow cells of the $Plg^{+/+}$ and $Plg^{-/-}$ mice, the cells were stimulated with RANKL (100 ng/ml) and M-CSF (100 ng/ml) for 7 days on the BioCoat™ Osteologic™ multi-test slides, which consisted of sub-micron synthetic calcium phosphate thin film coated onto various culture vessels (Becton Dickinson and Company, Bedford, MA USA). Then, the non-resorbed area of calcium phosphate film was visualized by using a method of von Kossa staining, as follows: After fixation of the cells in the culture with 5 % glutaraldehyde, the calcium phosphate film was treated with 5 % silver nitrate for 30 min. Then, the staining was developed with 5 % sodium carbonate in 25 % formalin. The stained film in each well was photographed under a light microscopy, then, the image was inverted to yield the negative image: black image represents the resorbed area in the calcium phosphate film.

Bone histology

Bone histomorphometry of tibia in 5-weeks old male $Plg^{+/+}$ and $Plg^{-/-}$ mice were performed. Each tibia was removed and fixed in 4 % paraformaldehyde for 2 days, and then demineralized with 10% EDTA for 14 days before embedding in paraffin. Paraffin-embedded tissue was serially sectioned at 4-7-μm distances. Then, the sections were stained with Hematoxylin-Eosin (H-E) and TRAP by using TRAP kit (Sigma- Aldrich, St Louis, MO USA).

For the quantitative evaluation of the intensity of TRAP-staining of bone marrow tissue in decalcified sections of tibia from the $Plg^{+/+}$ and $Plg^{-/-}$ mice, the TRAP-stained images obtained from separate fields on the

specimens (n=6) were analyzed by using ImageJ.

Measurement of bone mineral density

Bone mineral density (BMD) was measured as described by Kanazawa et al and Nishiwaki T et al (18,19). BMD of the proximal tibia of the $Plg^{+/+}$ and $Plg^{-/-}$ mice at the indicated time was evaluated by using peripheral quantitative computed tomography with a fixed x-ray fan beam of 50-μm spot size, at 1 mA and 50 kVp (LaTheta LCT-100S; Aloka, Tokyo, Japan).

RNA isolation and quantitative RT-PCR

Total RNA was extracted as previously described (6). First-strand cDNA was synthesized from total RNA by using the PrimeScript RT reagent Kit (Takara). Quantitative RT-PCR (qRT-PCR) was performed on the IQ5 real-time PCR detection system (Bio-Rad, CA, USA) with SYBR Green technology on cDNA generated from the reverse transcription of purified RNA. The 2 step PCR reactions were performed as 92℃ for 1s and 60℃ for 10 sec. OPG mRNA expression was normalized against GAPDH mRNA expression using the comparative cycle threshold method. We used the following primer sequence: OPG, 5'-CAATGGCTGGCTTGGTTTCATAG-3' and 5'-CTGAACCAGACATGACAGCTGGA-3'; GAPDH, 5'-TGTGTCCGTCGTGGATCTGA-3' and 5'-TTGCTGTTGAAGTCGCAGGAG -3'

Western blot analysis

We performed a Western blot analysis for detection of OPG, phospho-ERK1/2, phospho-p38 MAPK, ERK1/2, and p38 MAPK as previously described (20). We detected OPG, phospho-ERK1/2, phospho-p38 MAPK, ERK1/2, and p38 MAPK by incubation with a polyclonal OPG antibody (rabbit IgG, from Gene Tex, Inc. CA, USA), anti-phospho-ERK1/2 antibody (Cell Signaling Technology, Danvers, MA, USA), anti-phospho-p38 MAPK antibody (Cell Signaling Technology, Danvers, MA, USA), anti-ERK1/2 antibody (Cell Signaling Technology, Danvers, MA, USA), and anti-p38 MAPK antibody (Cell Signaling Technology, Danvers, MA, USA).

Measurement of alkaline phosphatase activity

We measured alkaline phosphatase (ALP) activity as previously described (20). Primarily cultured OBs were cultured for 14 day with differentiation media (media supplemented with 10 mM β-glycerophosphate and 10 nM dexamethasone and 50 μg/ml ascorbic acid) in 6-well plates. After 14 days, cells were then washed, and proteins in cells were extracted with a lysis

buffer (10 mM Tris-HCl, pH 7.5, 0.1 % Triton X-100). ALP activity was determined using *p*-nitro phenyl phosphate (Sigma-Aldrich Stein-heim, Germany) as a substrate.

Statistical analysis

All data are expressed as mean±SEM. The significance of the effect of each treatment (P <0.05) was determined by analysis of variance (ANOVA) followed by the Student Newman-Keuls test.

Results

Histological and radiological evaluation of the status of endochondral ossification in Plg-deficient mice

The bone mineral density (BMD) in the $Plg^{+/+}$ and $Plg^{-/-}$ mice at 4 to 20 weeks were radiologically assessed using peripheral quantitative computed tomography. Intriguingly, the trabecular BMD in tibia from the $Plg^{-/-}$ mice was significantly lower than that from the $Plg^{+/+}$ mice at 4 to 6 weeks after birth (Fig. 1A). In addition, the cortical BMD in tibia from the $Plg^{-/-}$ mice was significantly lower than that from the $Plg^{+/+}$ mice at 4 to 18 weeks after birth (Fig. 1B). The decrease of cortical BMD seemed to parallel that of the body weight-decrease in the $Plg^{-/-}$ mice at 4 to 18 weeks after birth (Fig. 1B and 1C). Next, the status of endochondral ossification in tibia from the $Plg^{+/+}$ and $Plg^{-/-}$ was histologically compared to clarify the effect of the fibrinolytic system in bone metabolism. As shown in Figure 1D, H-E staining of decalcified section of tibia from the 5-week old mice showed that the layer of chondrocytes and trabecular bone formation in the medullary cavities were observed in both $Plg^{+/+}$ and $Plg^{-/-}$ mice. The TRAP-staining of the decalcified section of the tibias from the 5-week old mice revealed that the area of TRAP-positive bone marrow tissue in the tibias from the $Plg^{-/-}$ mice was significantly larger than that of the tissue from the $Plg^{+/+}$ mice (Fig. 1E). In addition, the intensity of the TRAP-staining on the decalcified sections of bone marrow tissue in the $Plg^{+/+}$ and $Plg^{-/-}$ mice was quantitatively evaluated as described in the Materials and Methods. As shown in Fig. 1F, the intensity of TRAP-staining on decalcified sections of bone marrow tissue in tibias from the $Plg^{-/-}$ mice was much stronger than in those from the $Plg^{+/+}$ mice.

The effect of the Plg-deficiency on the osteoclastogenesis of bone marrow-derived cells

We evaluated how the fibronolytic system affects OC differentiation and function. The pre-OCs population in bone marrow-derived cells from the $Plg^{+/+}$ and Plg^{-}

$^{-/-}$ mice were respectively evaluated after stimulation with RANKL and macrophage colony-stimulating factor (M-CSF). As shown in Figure 2A, many TRAP-positive multinucleated OCs were observed in bone marrow cell cultures derived from the $Plg^{-/-}$ mice tibia. Therefore, an up-regulation of the TRAP-positive cell number in the $Plg^{-/-}$ mice-derived bone marrow cell was observed (Fig. 2B). In addition, the bone resorption activity of OCs differentiated from bone marrow-derived cells was compared in the $Plg^{+/+}$ and $Plg^{-/-}$ mice. There was an up-regulation of the bone resorption activity of $Plg^{-/-}$ mice-derived bone marrow cells (Fig. 2C). Intriguingly, plasmin significantly inhibited the M-CSF- and RANKL-induced OC differentiation of bone marrow cells derived from the $Plg^{-/-}$ and $Plg^{+/+}$ mice (Fig. 2D).

Plasmin induced the OPG expression in OBs.

In order to clarify how plasmin suppresses osreoclastgenesis *in vivo*, we examined whether plasmin up-regulates the expression of OPG in OBs from the WT mice *in vitro* by qRT-PCR and a Western blot analysis. Plasmin clearly induced OPG expression in OBs from the WT mice (Fig. 3A, B). In addition, the effect of various plasmin inhibitors (α2AP; serine protease inhibitor, aprotinin; lysine analogue, epsilon amino caproic acid (EACA)) on plasmin-induced OPG expression was investigated. These plasmin inhibitors clearly abrogated the plasmin-induced OPG expression (Fig. 3C, D).

In addition, we examined the plasmin-stimulated phosphorylation of extracellular signal-regulated kinase 1/2 (ERK1/2) and p38 mitogen-activated protein kinase (MAPK) in order to determine whether plasmin activates ERK1/2 and p38 MAPK in OBs. Plasmin activated ERK1/2 and p38 MAPK in OBs (Fig. 3E). We also examined whether the ERK1/2 and p38 MAPK pathways are associated with the plasmin-induced expression of OPG in OBs by using the inhibitor of mitogen activated protein kinase kinase (MEK) and p38 MAPK (PD98059, SB203580). PD98059 and SB203580 attenuated plasmin-induced expression of OPG in OBs (Fig. 3F). These data suggest the plasmin induces OPG expression through the ERK1/2 and p38 MAPK pathways.

Moreover, qRT-PCR and a Western blot analysis revealed that the expression of OPG was suppressed in OBs from the $Plg^{-/-}$ mice (Fig. 3G, H), thus suggesting that the absence of plasmin may result in the acceleration of osteoclastogenesis of pre-OCs in accordance with the depletion of OPG-synthesis in OBs. On the other hand, there was no difference in the status of RANKL

mRNA expression in OBs from the $Plg^{+/+}$ and $Plg^{-/-}$ mice (data not shown). Moreover, plasmin induced OPG expression in $Plg^{-/-}$ OBs (Fig. 3I, J).

Effects of Plg-deficiency on the ability of OBs to induce osteoclastogenesis of RAW264.7 mouse monocyte/macrophage lineage cells

The status of OC differentiation of RAW264.7 mouse monocyte/macrophage lineage cells in co-culture with $Plg^{-/-}$ OBs was examined to clarify how Plg deficiency affects OBs function for osteoclastogenesis. The ability of $Plg^{-/-}$ OBs to induce OCs-differentiation of pre-OCs RAW264.7 cells was compared with $Plg^{+/+}$ OBs. The OBs were co-cultured with RAW264.7 cells under stimulation with the inflammatory mediators interleukin 1-β (IL-1β) or prostaglandin E_2 (PGE_2). Inflammatory mediators induce RANKL expression on OBs (21). The inflammatory mediators-induced RANKL expression on OBs was expected to induce the osteoclastogenesis of the co-cultured RAW264.7 cells. As shown in Figure 4A, IL-1β or PGE_2 increased the number of TRAP-positive multinucleated cells co-cultured with OBs. Intriguingly, the number of TRAP-positive multinucleated cells co-cultured with $Plg^{-/-}$ OBs lacking OPG expression was significantly higher than that co-cultured with $Plg^{+/+}$ OBs with or without IL-1β or PGE_2. In addition, the number of TRAP-positive multinucleated cells co-cultured with $Plg^{-/-}$ OBs was decreased by plasmin (Fig. 4B).

Effect of Plg-deficiency on the ALP activity in OBs

The ALP activity in $Plg^{-/-}$ OBs was compared with $Plg^{+/+}$ OBs under stimulation with OB-differentiation media as described in Materials and Methods. The absence of Plg did not affect the ALP activity in undifferentiated- and differentiated OBs (Fig. 5).

Rescue of the down-regulated BMD in Plg-deficient mice by the injection of plasmin

To clarify the effect of exogenous plasmin on bone formation *in vivo*, we evaluated the status of the BMD in the $Plg^{-/-}$ mice with or without plasmin injection. The plasmin injection clearly increased the trabecular BMD in the $Plg^{-/-}$ mice (Fig. 6A). However, the plasmin injection did not affect the cortical BMD and the weight in the $Plg^{-/-}$ mice (Fig. 6B and C).

Discussion

Fibrinolytic factors have been suggested to play an important role in bone

metabolism. PAs and PAI-1 are involved in bone resorption by OCs (22,23). However, the role of Plg/plasmin in bone metabolism was not precisely understood. This study showed that Plg/plasmin plays an important role in bone metabolism by regulating the function of both OBs and OCs.

The trabecular BMD in the tibias from the $Plg^{-/-}$ mice was significantly lower than that from the $Plg^{+/+}$ mice at 4 to 6 weeks after birth (Fig. 1A). In contrast, the cortical BMD in the tibias from the $Plg^{-/-}$ mice was significantly lower than that from the $Plg^{+/+}$ mice at 4 to 18 weeks after birth (Fig. 1B). Therefore, the decrease in the trabecular BMD in $Plg^{-/-}$ mice seemed to be transient, however, the decrease in the cortical BMD in the mice was consistently observed from the juvenile growth period to adulthood. In addition, the TRAP-staining of decalcified sections of tibias from the 5-week old mice revealed that the intensity of TRAP-staining of bone marrow tissue in the tibias from the $Plg^{-/-}$ mice was significantly stronger than that from the $Plg^{+/+}$ mice (Fig. 1E and F). Thus, the histoenzymatic assessment indicated that the OC-differentiation in bone marrow tissue of the $Plg^{-/-}$ mice might be more vigorously induced than that in the $Plg^{+/+}$ mice.

The binding of RANKL to its receptor RANK triggers intricate and distinct signaling cascades that control lineage commitment and osteoclasts activation (13). OPG inhibits osteoclasts formation and bone resorption by blocking RANKL/RANK interactions (14). The current study showed that plasmin increased the OPG expression in WT OBs (Fig. 3A-D). Moreover, the expression level of OPG was decreased in $Plg^{-/-}$ OBs compared to $Plg^{+/+}$ OBs (Fig. 3G, H), suggesting that absence of plasmin may result in an acceleration of OB-mediated osteoclastogenesis of pre-OCs in accordance with the depletion of OPG expression in OBs. In fact, the number of TRAP-positive multinucleated RAW264.7 cells co-cultured with $Plg^{-/-}$ OBs was significantly higher than that of the cells co-cultured with $Plg^{+/+}$ OBs (Fig. 4A). Intriguingly, plasmin significantly inhibited the M-CSF- and RANKL-induced OC-differentiation of bone marrow cells derived from the $Plg^{+/+}$ and $Plg^{-/-}$ (Fig. 2D), suggesting that plasmin might attenuate osteoclastogenesis by its some direct effects on pre-OCs. In addition, there was a larger population of pre-OC in bone marrow-derived cells from the $Plg^{-/-}$ mice in comparison to the $Plg^{+/+}$ mice (Fig. 2A, B and C). On the other hand, the level of ALP activity in $Plg^{-/-}$ OBs was similar to that in $Plg^{+/+}$ OBs (Fig. 5), thus suggesting that the bone-mineralizing activity of OBs in the $Plg^{-/-}$ mice might be comparable with that in the $Plg^{+/+}$ mice. Consequently, the $Plg^{-/-}$ mice display decreased bone mineral density in

accordance with the enhanced ability of OBs to induce osteoclastogenesis of pre-OCs, the loss of the direct and suppressive effect of plasmin on pre-OCs differentiating into mature OCs and the increased pre-OCs population in bone marrow cells. In fact, the injection of plasmin into the $Plg^{-/-}$ mice clearly rescued the diminished trabecular BMD during the juvenile growth period (Fig. 6).

Plasmin activates a latent transforming growth factor β (TGF-β) (24,25) trapped in extra cellular matrix (ECM) to induce an OPG expression in ECM-harbored OBs. The accelerated expression of OPG on OBs might result in the suppression of the OB-mediated osteoclastogenesis. It is under the investigation by us whether deficiency of activated TGF-β causes decreased bone mineral density and decreased body weight in $Plg^{-/-}$ mice. On the other hand, plasmin directly activates various intracellular signaling through annexin A2 in macrophage (26). Plasmin activates macrophages via the annexin A2 heterotetramer composed of annexin A2 and S100A10 with subsequent stimulation of Janus kinase JAK1/TYK2 signaling. JAK1/TYK2 leads to STAT3 activation, Akt-dependent nuclear factor kappaB (NF-κB) activation, and phosphorylation of ERK1/2 and p38 MAPK. Furthermore, inhibitors of JAK, p38 MAPK, and NF-κB revealed that these signaling pathways are indispensable for the plasmin-mediated tumor necrosis factor-a and IL-6 induction in the cells. In addition, angiostatin, a fragment of plasmin(ogen), is a ligand and an antagonist for integrin α9β1 (27). Angiostatin, representing the kringle domains of plasmin, alone did not induce the migration of chinese hamster ovary (CHO) cells, but simultaneous activation of the G protein-coupled protease-activated receptor (PAR)-1 with an agonist peptide induced the migration on angiostatin. These facts suggest that plasmin directly stimulates various cell-lineages without an indirect cell-stimulation through an activation of some growth factors such as TGF-β. We showed that plasmin activated ERK1/2 and p38 MAPK, and the inhibition of ERK1/2 and p38 MAPK attenuated plasmin-induced OPG expression (Fig. 3E, F). In addition, plasmin activated c-jun N-terminal kinase (JNK), but the inhibition of JNK did not attenuate plasmin-induced OPG expression (data not shown). These data suggest that plasmin induces OPG expression through ERK1/2 and p38 MAPK pathway. On the other hand, the time lag between the activation of p38 MAPK and ERK1/2 after the plasmin stimulation in OBs might depend on the hierarchy of ERK1/2 and p38 MAPK in the plasmin-induced signal transduction: The ERK1/2 might be the downstream target of p38 MAPK directly activated by plasmin

in OBs. Further investigations would be required to clarify the details.

The current results strongly suggest that the plasmin activity regulates both OBs and OCs function, and then plays an important role in the bone metabolism. These findings may provide new insights into the development of clinical therapies for the prevention of bone loss related disorders.

Acknowledgments

This work was supported by grants-in-aid for Young Scientists (B:21790097 to Y. Kanno) from the Ministry of Education, Culture, Sports, Science and Technology, Japan Society for the Promotion of Science and Grant-in-Aid for Strategic Medical Science Research Center from the Ministry of Education, Culture, Sports, Science and Technology of Japan, 2010-2014.

Reference

1. Braaten JV, Handt S, Jerome WG, Kirkpatrick J, Lewis JC, Hantgan RR. (1993) *Blood.* **81**, 1290-1299.
2. Lijnen HR, De Cock F, Van Hoef B, Schlott B, Collen D. (1994) *Eur J Biochem.* **224**, 143-149
3. Carmeliet P, Collen D. (1996) *Semin Thromb Hemost.* **22**, 525-542
4. Matsuno H, Ishisaki A., Nakajima K, Okada K, Ueshima S, Matsuo O, Kozawa O. (2003) *Blood.* **102**, 3621-3628.
5. Kanno Y, Kuroki A, Minamida M, Kaneiwa A, Okada K, Tomogane K, Takeuchi K, Ueshima S, Matsuo O, Matsuno H. (2008) *Thromb Res.* **123**, 336-341.
6. Kanno Y, Hirade K, Ishisaki A, Nakajima K, Suga H, Into T, Matsushita K, Okada K, Matsuo O, Matsuno H. (2006) *J Thromb Haemost.* **4**, 1602-1610.
7. Kanno Y, Kuroki A, Okada K, Tomogane K, Ueshima S, Matsuo O, Matsuno H. (2007) *J Thromb Haemost.* **5**, 2266-2273.
8. Kanno Y, Kaneiwa A, Minamida M, Kanno M, Tomogane K, Takeuchi K, Okada K, Ueshima S, Matsuo O, Matsuno H. (2008) *J Invest Dermatol.* **128**, 2792-2797
9. Kanno Y, Kawashita E, Minamida M, Kaneiwa A, Okada K, Ueshima S, Matsuo O, Matsuno H. (2010) *Am J Pathol.* **176**, 238-245.

10. Daci E, Everts V, Torrekens S, Van Herck E, Tigchelaar-Gutterr W, Bouillon R, and Carmeliet G. (2003) *J Bone Miner Res.* **18**, 1167-1176.

11. Daci E, Verstuyf A, Moermans K, Bouillon R, Carmeliet G. (2000) *J Bone Miner Res.* **15**, 1510-1516.

12. Furlan F, Galbiati C, Jorgensen NR, Jensen JE, Mrak E, Rubinacci A, Talotta F, Verde P, Blasi F. (2007) *J Bone Miner Res.* **22**, 1387-1396.

13. Wada T, Nakashima T, Hiroshi N, Penninger JM. (2006) *Trends Mol Med.* **12**, 17-25.

14. Hofbauer LC, Heufelder AE. (2001) *J Mol Med.* **79**, 243-253.

15. Li J, Sarosi I, Yan XQ, Morony S, Capparelli C, Tan HL, McCabe S, Elliott R, Scully S, Van G, Kaufman S, Juan SC, Sun Y, Tarpley J, Martin L, Christensen K, McCabe J, Kostenuik P, Hsu H, Fletcher F, Dunstan CR, Lacey DL, Boyle WJ. (2000) *Proc Natl Acad Sci U S A.* **97**, 1566-1571.

16. Ploplis VA, Carmeliet P, Vazirzadeh S, Van Vlaenderen I, Moons L, Plow EF, Collen D. (1995) *Circulation.* **92**, 2585-2593.

17. Suda T, Jimi E, Nakamura I, Takahashi N. (1997) *Methods Enzymol* **282**, 223–235

18. Kanazawa S, Ota S, Sekine C, Tada T, Otsuka T, Okamoto T, Sønderstrup G, Peterlin BM. (2006) *Proc Natl Acad Sci U S A.* **103**, 14465-14470.

19. Nishiwaki T, Yamaguchi T., Zhao C, Amano H, Hankenson KD, Bornstein P, Toyama Y, Matsuo K. (2006) *J Bone Miner Res.* **21**, 596-604.

20. Kanno Y, Into T, Lowenstein CJ, Matsushita K. (2008) *Cardiovasc Res.* **77**, 221-230.

21. Nakashima T, Kobayashi Y, Yamasaki S, Kawakami A, Eguchi K, Sasaki H, and Sakai H. (2000.) *Biochem. Biophys. Res. Commun.* **275**, 768-775

22. Daci E, Udagawa N, Martin TJ, Bouillon R, Carmeliet G. (1999) *J Bone Miner Res.* **14**, 946-952.

23. Everts V, Daci E, Tigchelaar-Gutter W, Hoeben KA, Torrekens S, Carmeliet G, Beertsen W. (2008) *Bone.* **43**, 915-920.

24. Thirunavukkarasu K, Miles RR, Halladay DL, Yang X, Galvin RJ, Chandrasekhar S, Martin TJ, Onyia JE. (2001) *J Biol Chem.* **276**, 36241-36250.

25. Lyons RM, Gentry LE, Purchio AF, Moses HL. (1990.) *J Cell Biol.* **110**, 1361-1367.

26. Li Q, Laumonnier Y, Syrovets T, Simmet T. (2007) *Arterioscler Thromb Vasc Biol.* **27**, 1383-1389

27. Majumdar M, Tarui T, Shi B, Akakura N, Ruf W, Takada Y. (2004) *J Biol Chem.* **279**, 37528-37534.

Legends to Figures

Figure 1. ***The bone histomorphometry and bone mineral density in Plg deficient mice***

(A) Trabecular BMD in the proximal tibia of male $Plg^{+/+}$ and $Plg^{-/-}$ mice was obtained from pQCT measurement (n=13). (B) Cortical BMD in the proximal tibia of the $Plg^{+/+}$ and $Plg^{-/-}$ mice was obtained from pQCT measurement (n=13). (C) The growth curves of the $Plg^{+/+}$ and $Plg^{-/-}$ mice (n=13). (D and E) Bone histomorphometry of tibia in 5-week-old male $Plg^{+/+}$ and $Plg^{-/-}$ mice (D: hematoxylin and eosin, E: TRAP). In D, the layer of chondrocytes and trabecular bone formation in the medullary cavities were observed in both $Plg^{+/+}$ and $Plg^{-/-}$ mice. In E, the TRAP-positive area in the bone marrow tissue of the tibias from $Plg^{-/-}$ mice was much larger than that in the tissue specimens obtained from $Plg^{+/+}$ mice. (F) The intensity of TRAP-staining on the decalcified sections of bone marrow tissue in the $Plg^{+/+}$ and $Plg^{-/-}$ mice was quantitatively evaluated as described in the Materials and Methods (n=6). The intensity of TRAP-staining on the sections from the $Plg^{-/-}$ mice was much stronger than that of sections from $Plg^{+/+}$ mice. The data represent the mean ± SEM. *, $P<0.01$; #, $P<0.05$.

Figure 2. ***The effect of the Plg deficiency on osteoclastogenesis and the OCs-function***

(A) Bone marrow cells from the $Plg^{+/+}$ and $Plg^{-/-}$ mice were cultured for 3 days in the absence or presence of RANKL (100 ng/ml) and M-CSF (100 ng/ml). Mature OCs were identified as TRAP positive multinucleated cells. The magnified image of boxed area was showed on the right of the original image. The arrowheads indicate osteoclasts. (B) The number of TRAP-positive multinucleated cells in (A) was determined from three different cultures. (C) The bone resorption activity of OCs differentiated from bone marrow-derived cells obtained from the $Plg^{+/+}$ and $Plg^{-/-}$ mice was compared. Bone marrow-derived cells from the $Plg^{+/+}$ and $Plg^{-/-}$ mice were cultured on the BioCoat™ Osteologic™ multi-test slides, which consisted of sub-micron synthetic calcium phosphate thin film coated onto various culture vessels, for 7 days in the presence of RANKL (100 ng/ml) and M-CSF (100 ng/ml) (n=4). Next, the resorbed areas of the calcium phosphate film were visualized as described in the Materials and Methods. The histogram on the right panels shows quantitative representations of bone resorption obtained from densitometry analysis. The densitometry results were expressed as the mean density. (D) Bone marrow cells from the $Plg^{+/+}$ and $Plg^{-/-}$ mice were cultured for 3 days in the presence of M-CSF (100 ng/ml). Some cells were cultured in the presence or absence of RANKL (100

ng/ml) or plasmin (1 μg/ml) as indicated. The number of multinucleated TRAP positive cells was determined from four different cultures. The data represent the mean ± SEM. *, $P<0.01$; **, $P<0.05$.

Figure 3. ***Plasmin induced the OPG expression in OBs.***

(A to D) OBs from the WT mice were cultured for 24 hours in either the absence or presence of plasmin (1 μg/ml). Plasmin-induced expression of OPG gene in OBs from the WT mice was evaluated by qRT-PCR (A) or a Western blot analysis (B). In C and D, some cultures were further treated with plasmin inhibitors: α2AP (200 nM), EACA (25 mM), and aprotinin (10 μg/ml). Then, the expression of OPG mRNA in OBs from the WT mice was measured by qRT-PCR (C) or a Western blot analysis (D). (E) OBs from the WT mice were stimulated with 1 μg/ml plasmin for the indicated periods. Phosphorylation of ERK1/2 and p38 MAPK were evaluated by a Western blot analysis using antibodies to ERK1/2 and p38 MAPK. (F) OBs from the WT mice were pretreated with 30 μM PD98059 or 30 μM SB203580 for 60 min and then stimulated with 1 μg/ml plasmin for 24 hours. The expression of OPG in OBs from the WT mice was evaluated by a Western blot analysis. In G and H, the OPG expression in OBs from the $Plg^{+/+}$ and $Plg^{-/-}$ mice was evaluated by qRT-PCR (G) or a Western blot analysis (H). In I and J, OBs from the $Plg^{-/-}$ mice were cultured for 24 hours in the absence or presence of plasmin (1 μg/ml). Then, the OPG expression in OBs from the $Plg^{-/-}$ mice was evaluated by qRT-PCR (I) or a Western blot analysis (J). The data represent the mean of 3 individual experiments ± SEM. *, $P<0.01$; **, $P<0.05$.

Figure 4. ***Effects of Plg-deficiency on the ability of OBs to induce osteoclastogenesis of Raw 264.7 cells***

(A) Raw264.7 cells and OBs from the $Plg^{+/+}$ and $Plg^{-/-}$ mice were co-cultured for 3 days in the absence or presence of IL-1β or PGE_2. (B) Raw264.7 cells and OBs from the $Plg^{-/-}$ mice were co-cultured for 3 days in the absence or presence of plasmin. Mature OCs were identified as multinucleated TRAP positive cells. The number of multinucleated TRAP positive cells was determined from six different cultures. The data represent the mean ± SEM. *, $P<0.01$.

Figure 5. ***Effect of Plg-deficiency on the ALP activity in OBs***

ALP activity in OBs from the $Plg^{+/+}$ and $Plg^{-/-}$ mice was evaluated (n=4). The data represent the mean ± SEM. *, $P<0.01$.

Figure 6. ***Rescue of the down-regulated BMD in Plg-deficient mice by the injection of plasmin***

Intraperitoneal injection with saline or plasmin (1 mg/kg) in the 5-week-old male $Plg^{-/-}$ mice was carried out weekly for up to 3 weeks. Then, the trabecular BMD (A), the cortical BMD (B), and the weight (C) in the male $Plg^{-/-}$ mice were measured by pQCT (n=3). The data represent the mean ± SEM. *, $P<0.01$.

Kanno et al 2010, Figure 1

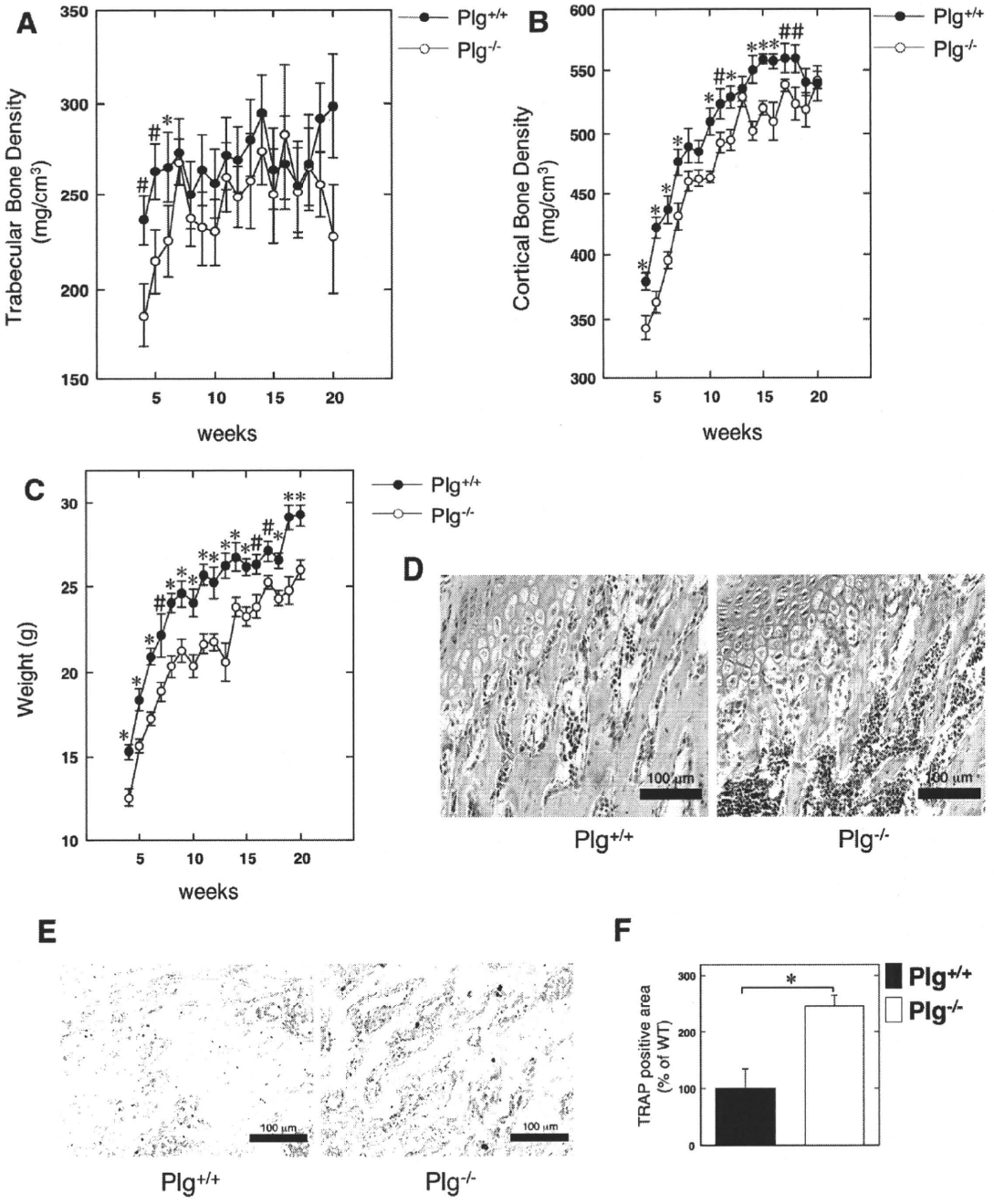

Kanno et al 2010, Figure 2

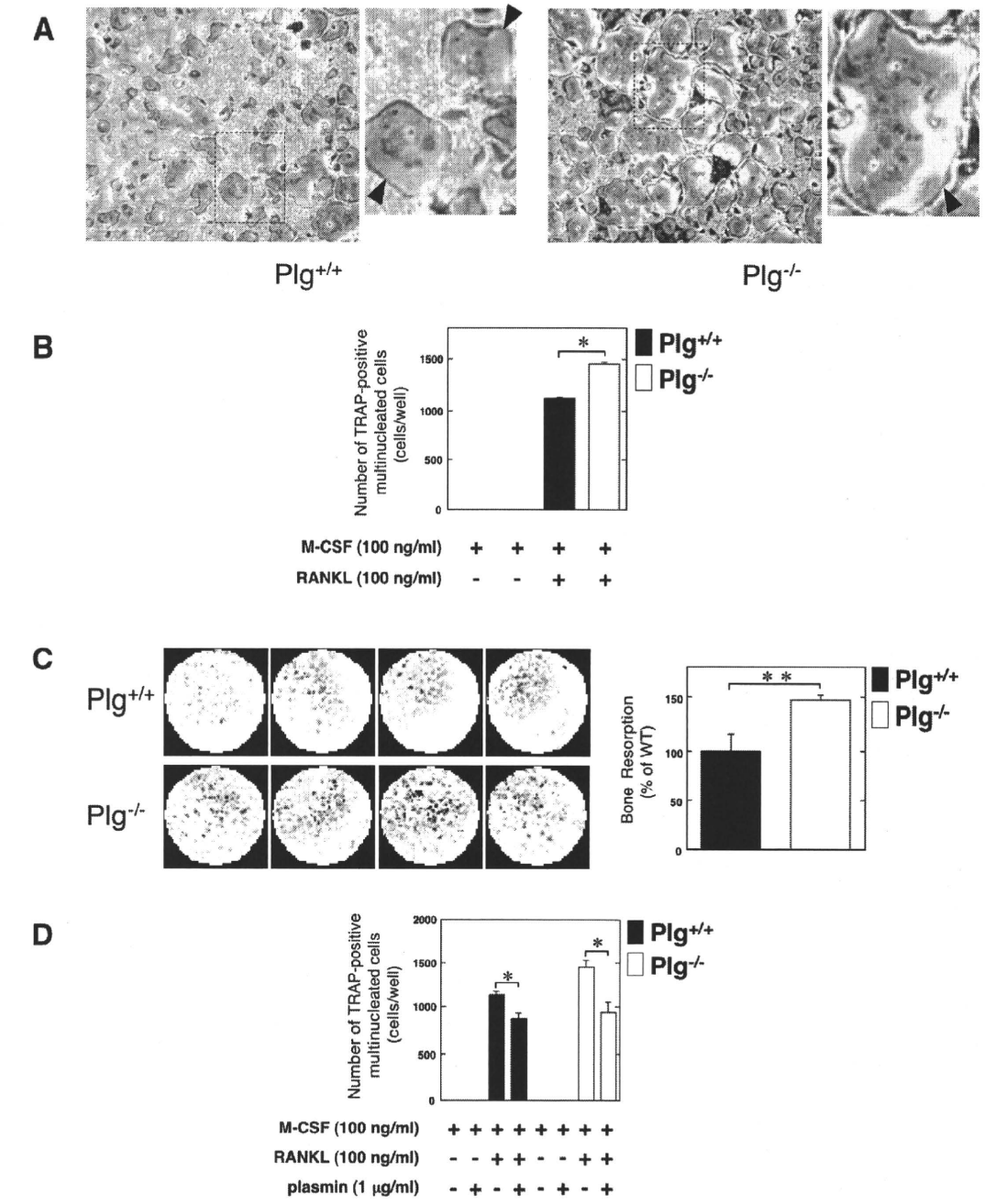

Kanno et al 2010, Figure 3

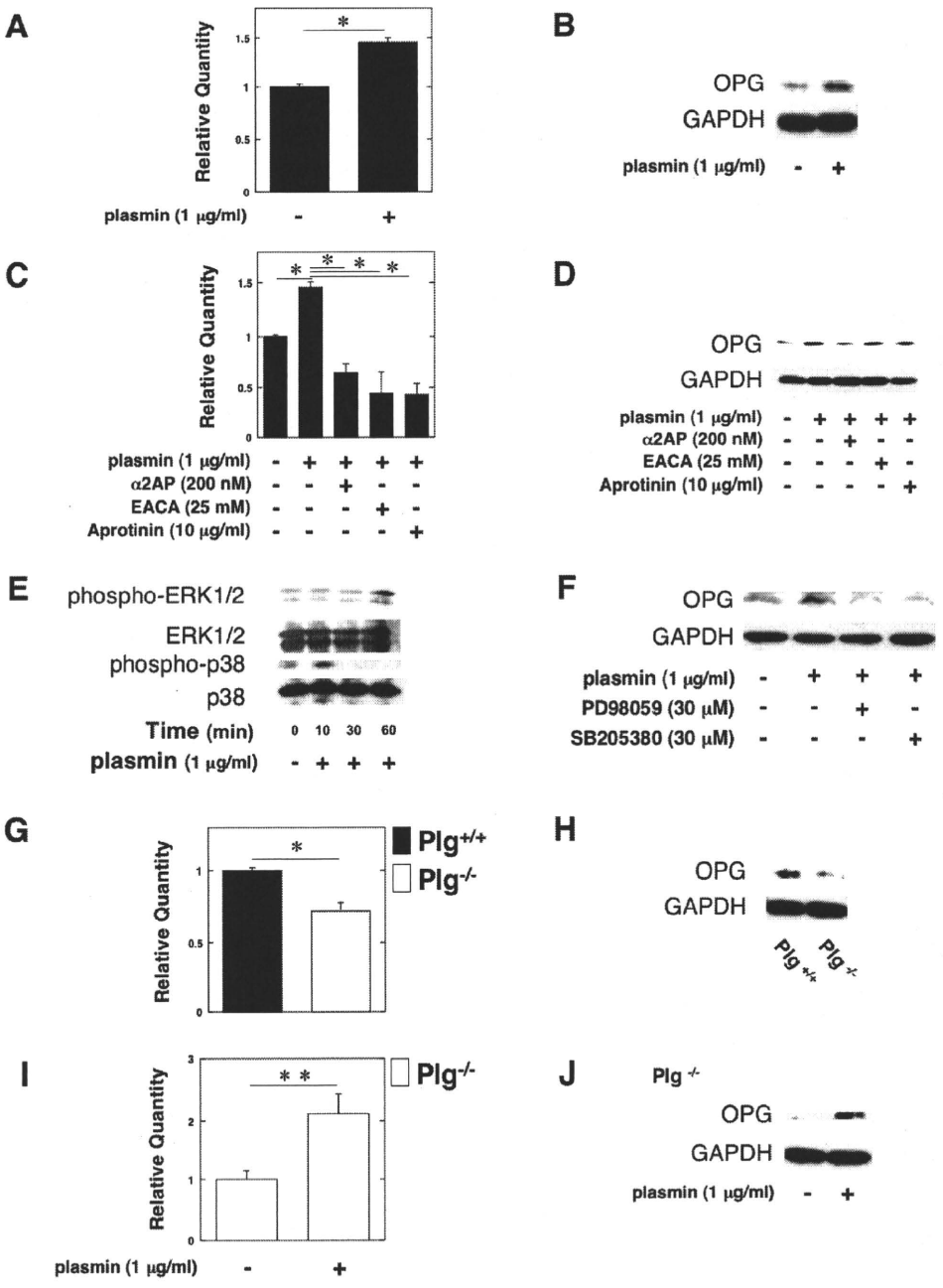

Kanno et al 2010, Figure 4

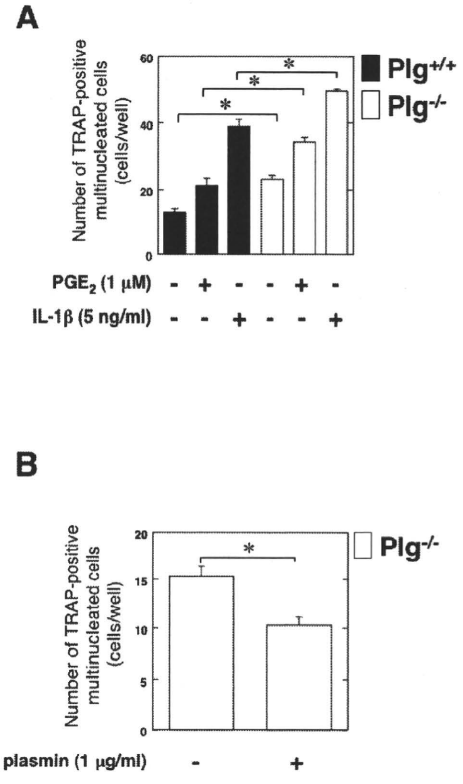

Kanno et al 2010, Figure 5